Oct 18th, 12:00 AM

Cold-formed Steel Sections for Transmission Towers

David Odaisky

Dimos Polyzios

Glenn Morris

Twelfth International Specialty Conference on Cold-Formed Steel Structures
St. Louis, Missouri, U.S.A., October 18-19, 1994

COLD-FORMED STEEL SECTIONS FOR TRANSMISSION TOWERS

David Odaisky[1] Dimos Polyzois[2] Glenn Morris[3]

Introduction

Hydro-electric transmission towers are traditionally built using hot-rolled angles. However cold formed angles are becoming more popular as replacements for hot-rolled angles, especially in the smaller angle sizes. In addition to conventional 90° angles, a wide range of shapes can be produced, in sizes to suit individual project requirements. In particular, cold-forming can be used to provide stiffening lips to prevent local buckling of thin wide elements, to optimize shapes so that longer unbraced lengths can be used, and to create shapes such as 60° angles for triangular towers.

A research project was carried out at the University of Manitoba to examine the axial compressive load capacity of a number of cold-formed shapes suitable for transmission tower construction. Test parameters included: five different cross-sections, two steel grades, three different slenderness ratios, and three temperature levels. Specimens were tested in setups designed to simulate end conditions representative of actual web members by loading through single legs bolted to gusset plates. A number of specimens were loaded concentrically with hinged end conditions. Three special test setups were constructed to accommodate the wide range of sections, which varied from 552 mm to 8200 mm in length. A total of 189 static tests were performed. Test results were compared to ultimate loads obtained from the Canadian Standards such as CAN/CSA-S136-M89, Cold Formed Steel Structural Members, and CAN/CSA-S37-M86, Antennas, Towers, and Antenna Supporting Structures, as well as to loads predicted by the ASCE Manual 52, Guide for Design of Steel Transmission Towers, and the ECCS Recommendations for Angles in Lattice Transmission Towers.

1. Graduate Student, Department of Civil and Geological Engineering, University of Manitoba,Winnipeg, MB., Canada, R3T 5V6
2. Associate Professor, Department of Civil and Geological Engineering, University of Manitoba,Winnipeg, MB., Canada, R3T 5V6
3. Professor, Department of Civil and Geological Engineering, University of Manitoba,Winnipeg, MB., Canada, R3T 5V6

Experimental program

A total of 189 galvanized, cold-formed steel sections were tested under static compression. Test parameters included five different shapes, two steel types, three temperatures, and three slenderness ratios. The parametric variations are listed in Table 1. The section properties for each shape are listed in Table 2. These properties are based on the average recorded dimensions for each shape, with the galvanizing thickness deducted.

One set of specimens were produced by SAE of Italy using ASTM A715 grade 60 steel. The other set of specimens were produced locally using CSA G40.21 grade 300W steel. Steel thickness was specified as 4.5 mm for the G40.21 steel, and 4.0 mm for the A715 steel, except for the channel specimens which were specified as having a thickness of 5.0 mm.

The specimens were tested at three different temperature levels. Tests were performed at temperatures of -50 °C, 0 °C, and room temperature (approximately 20 °C to 24 °C).

Slenderness ratios of 40, 100, and 200 were considered in order to represent a wide range of potential compression members. The exact slenderness ratios of the specimens varied, so these ratios are referred to as the nominal slenderness ratios.

The following specimen designation system was used in this investigation: (H)XX - NN - II. The first letter, H is used to identify those specimens made of G40.21-300W steel, and is only used with these shapes. XX identifies the specimen shape as follows: BA for plain angles, BB for lipped angles, BC for 60° angles, BG for T-shaped sections, and BN for back-to-back channels. NN refers to the nominal slenderness ratio of the specimen, and is either 40, 100, or 200. II refers to the individual specimen identification within each shape and slenderness group. Under this system, each specimen has a unique identifying number.

End Supports

The specimen supports were designed to simulate end conditions experienced in tower construction. The angle sections (BA, HBA, BB, HBB, BC, HBC) were loaded through one leg, connected to gusset plates. Angles connected in this fashion are subjected to both eccentric loading, and end restraint. A number of angles were testeed with both legs bolted to the supports. These conditions were used to simulate typical supports for tower leg members. The gusset plate used to connect the angle shaped specimens to the supports is shown in Fig. 1. A channel extension was utilized in order to allow for easy replacement in the event of damage to the gusset plate.

The back-to-back channel sections were loaded concentrically by bolting these sections to gusset plates located between the webs. The ends of the gusset plate were hinged to allow rotation of the specimens about the weak axis. The channels were bolted back-to-back quarter length points with 1/2" (12.7 mm) thick spacer plates complete with two 3/8" (9.5 mm) diameter bolts at each plate. The gusset plate used to connect the back-to-back channels in Test Setup #1 is shown in Fig.2. A similar gusset plate was used for the channel specimens in Test Setup # 2 and # 3, as shown in Fig.3.

The double web T-shaped BG specimens were also loaded concentrically by bolting these to a gusset plate located between the two webs. The flanges of the section were also connected to the gusset plate through small clip angles. The gusset plate used to connect the BG specimens to the support is shown in Fig. 4. In Setup #2, the BG specimens were first tested without hinged end conditions. Subsequently, it was decided that in Setups #1 and #3, these specimens would be tested using the details illustrated in Figs.2 and 3. The hinge supports were oriented in a way which allowed rotation about the axis of symmetry of the section.

All connections were made with 5/8" (15.9 mm) diameter A325 bolts. The number of bolts used for each shape was determined by preliminary capacity calculations. The connections were designed to exceed the predicted buckling strength, but were not overdesigned. Therefore, the number of bolts used to connect each particular shape varied, depending on the member length.

Experimental setups

Three experimental setups were required to accommodate the variety of shapes and lengths used in this investigation. The first test setup consisted of an 810 mm x 950 mm x 2440 mm cold chamber with 200 mm diameter access holes at the top and bottom to accommodate the loading system. Pipe extensions were connected at the top to the hydraulic actuator, and at the bottom to the fixed base. The gusset plates were then connected to the pipe extensions. Specimens ranging in length from 552 mm to 1950 mm were tested at three temperature levels in this cold chamber.

The second setup consisted of a new custom-built cold chamber measuring 1050 mm x 1420 mm x 5300 mm. This chamber was installed in a reaction frame consisting of two 8230 mm tall steel columns, with cross beams at the top to react against the top of the specimens. A hydraulic jack resting on the structural floor was used to apply the load to the specimen. As in Setup #1, variable length pipe extensions were utilized to transfer loading to the specimens. Specimens ranging in length from 2000 mm to 4500 mm in length were tested in this setup at three temperature levels.

A third test setup was required to test the long T-shaped and back-to-back channel sections (BG-200, and BN-200). These specimens were approximately 8200 mm long, and were tested horizontally, at room temperature only. The setup consisted of two end blocks tied together by a system of dywidag bars. Loads were applied with two hydraulic jacks located between one end of the specimen, and the reaction block.

All specimens were loaded gradually by increasing the stroke of the loading pistons. The displacement was increased until the measured loads reached a maximum level. Tests were terminated when the measured loads decreased to approximately 90% of the ultimate load. A load cell was used to measure the applied loads. The relative vertical displacement between the ends of the specimen were measured by monitoring the stroke of the loading actuator. A thermocouple was used to monitor the temperature in the cold chambers. Lateral and rotational displacements were monitored by four motion transducers located at midheight of the specimen. Data was monitored and recorded by a Hewlett Packard data acquisition system.

Test results and discussion

Material Properties

Standard tension coupon tests were performed on coupons cut from specimens identical to those used in the investigation (Abdel Rahim A.B. et al. 1994). Table 3 lists the results from tension tests performed at room temperature on galvanized and ungalvanized standard coupons cut from flat portions of the specimens. The results from tests on ungalvanized A715 and G40.21 steel specimens confirmed the specified yield strengths of 415 MPa and 300 MPa, respectively.

Member Behaviour

The mean experimental results from all static axial compression tests, at all temperatures are shown in Table 4. The average of all ultimate experimental failure loads for static tests performed at 0 °C was 1.3% higher than at the average results from tests conducted at room temperature. Also, the average of all tests performed at -50 °C was 3.8% higher than the average results from tests conducted at room temperature. The largest increase in strength at both cold temperatures occurred for the lowest slenderness level for each shape. Specimens with nominal slenderness ratios of 40 demonstrated an average increase of 7.4% at -50 °C compared to room temperature results, whereas the longest members (L/r=200) showed an average increase of only 2%.

Theoretical ultimate load capacities were calculated for the full range of slenderness ratios for each shape using various design methods. Average section properties and measured yield strengths were considered in the analysis. Where applicable, the specified resistance factors were set equal to unity to obtain the "ultimate capacity". The actual slenderness ratios used in the calculations varied slightly from the nominal slenderness ratios. In calculating the actual slenderness ratios, the length was taken as the distance between the centroids of bolts at each end of the member, with the exception that for gusset plates with hinges, the length was taken as the distance between the hinges.

The capacities for the plain 90° angles were calculated using the following standards and specifications:

- CSA-S136-M89 standard for Cold-Formed Steel Structural Members (CSA, 1989)
- CSA-S37-M86 Antennas, Towers, and Antenna-Supporting Structures (CSA, 1986)
- ASCE Manual 52 "Guide for Design of Steel Transmission Towers" (ASCE, 1988)
- ECCS Recommendations for Angles in Transmission Towers (ECCS, 1985).

All four of these design guidelines provide methods for the design of plain angles loaded eccentrically through one leg, and account for end fixity in various ways. The ultimate capacities of the remaining sections were calculated using the CSA-S136 Standard and the ASCE Manual 52. The recent amendment no. 12 of the CSA-S37-M86 Standard was also used to calculate capacities for the 60° angles. The predicted failure loads for each shape are shown along with the experimental results in Table 4. The ultimate capacity of the five sections tested, obtained through the various standards and specifications is shown as a function of their

slenderness ratio in Figs. 5 to 13. The experimental results are also shown in those figures. A brief discussion of the results is given in the following section.

Plain angles

The experimental test results along with the predicted capacities for the BA and HBA sections are shown in Figs. 5 and 6, respectively. Since angles are very commonly used in the construction of transmission towers, the current standards and specifications devote considerable coverage on the design of such members.

The ASCE Manual 52, for example, bases the design of eccentrically loaded angles on an effective length approach. Depending on the member slenderness, number of bolts and type of connection, an effective length is specified which accounts for the eccentricity and end fixity. Local buckling of angles is accounted for by specifying a reduced critical stress, dependent on the width-thickness ratio and yield strength of the member. The buckling stress of the member is based on Euler strength in the elastic range, and the Structural Stability Research Council (SSRC) formula in the inelastic range.

The Canadian Standard CSA-S136 includes a clause (6.7.4) for the design of single angles loaded through one leg. This clause combines the effects of bending and twisting to provide a reduced equivalent slenderness ratio. The number of bolts in the connection is accounted for in determining the flexural buckling effective length, and the width-thickness ratio is considered in the torsional buckling effective slenderness ratio. Local buckling is accounted for by specifying reduced effective areas, depending on the width-thickness ratio, plate buckling coefficient (k), and the stress in the element. The column buckling stress is calculated using the same SSRC curve utilized in ASCE Manual 52, except that the Euler buckling stress is reduced by a factor of 0.833.

The CSA-S37 approaches the design of eccentrically loaded angles by specifying different effective length coefficients, and performance factors depending upon the slenderness ratio, and the number of bolts utilized. Local buckling is accounted for by specifying a reduced critical strength, similar to the method used by Manual 52. The column buckling stress is obtained from the curves provided by CSA Standard S16.1.

The European Recommendation for Angles in Lattice Transmission Towers use a similar approach to the design of angles bolted through one leg as specified in Manual 52. The effective length of the member is modified depending on end conditions, and slenderness ratios. Local buckling is accounted for by calculating a reduced effective yield stress depending on the width-thickness ratio and yield strength of the member. The approach is slightly different than that of Manual 52 in that different reductions are applied to cold-formed angles than to hot-rolled angles. The approach accounts for the reduced torsional stiffness of cold-formed angles due to the lack of a heel and fillet, and accounts for the increased yield strength at the corners of cold-formed angles due to the forming process. A lower buckling strength is applied to cold-formed angles with low slenderness and width-thickness ratios. At higher slenderness and width-thickness ratios the two types of angles are treated the same. In contrast, Manual 52, and S37 do not differentiate between hot-rolled and cold-formed angles in this regard.

The predicted capacity curves indicate a shift at a slenderness ratio of 150. This is based on the assumption that two or more bolts are used in the connections when the slenderness ratio is less than 150. Angles connected with more than one bolt at the ends experience greater end restraint, and this is reflected in the predicted capacities. The test specimens with nominal slenderness ratios of 40 and 100 were connected with two bolts at each end, and the specimens with L/r=200 had only one bolt at each end. The different design methods provided similar results, which, in general, were acceptable. The most notable discrepancies between predicted and test results occurred for the HBA-40 and BA-40 specimens which failed when distortions developed in the bolted legs near the gusset plates. The predicted loads overestimated some of these test results. For example the predicted ultimate load for the HBA-40 specimens, calculated using CSA Standard S37, was 37% higher than the mean experimental loads. It should be noted, however, that for the CSA-S37 approach, the resistance factor is modified to account for the eccentricity of load. Setting it equal to one, as used in the figures, results in unconservative "ultimate" predicted loads.

60° angles

The test results of 60° angles (BC and HBC sections) are shown in Figs. 7 and 8 along with the predicted ultimate. These sections were also bolted with two bolts at each end for slenderness ratios of 40, and 100, and with one bolt at L/r=200. As observed for the BA and HBA specimens, the shortest specimen capacities were overestimated in many cases. The capacities of the HBC-100 specimens were also overestimated.

Lipped angles

The results for the lipped angles (BB and HBB specimens) are shown in Figs. 9 and 10. Although the method of analysis provided by Clause 6.7.4 of the CSA Standard S136-M89 was developed for plain unstiffened angles, the method, when applied to stiffened angles generally provided good results except that the capacities of the HBB-40 and HBB-100 sections were overestimated.

Back-to-back channels

The test results and predicted loads for the BN and HBN sections are shown in figures 11 and 12. CSA Standard S136-M89 applies to specimens with thicknesses up to 4.5 mm, and specifies that CSA Standard S16.1 be utilized for sections greater than 4.5 mm in thickness. The BN sections were 5.0 mm thick, and the HBN sections were 4.5 mm thick. For comparison purposes, the results from both standards are shown for each of the BN and HBN specimens. The curves are based on the flexural buckling capacity and neglect torsional buckling, consistent with the observed failure modes.

Some inconsistency was observed between the test results and predicted loads for the back-to-back channels (BN-100, HBN 100, and BN-200 sections in particular). ASCE Manual 52 overestimated their ultimate capacity by as much as 56% for the longest specimens. One possible reason for this inconsistency was that Manual 52 does not account for the reduced rigidity of separate sections connected together at discrete locations. The CSA-S136 Standard provided better ultimate load predictions due to the fact that it specifies a reduction in the Euler elastic buckling stress by a factor of 0.833. This reduction is applied to ensure an adequate

margin of safety as the slenderness ratio increases into the elastic range, and it also accounts for possible member imperfections which prevent the member from reaching the full Euler flexural buckling strength. CSA-S136 also reduces the member capacity to account for the back-to-back connection spacing. It should be noted that the sections with L/r=200 were 8200 mm long, and had initial out of straightness of up to 13 mm.

T-shaped sections

Test results and predicted capacities for the BG specimens are shown in Fig. 13. These specimens were assumed to be loaded concentrically by the gusset plate connection. It was also assumed that the gusset plate connection provided some degree of warping restraint by virtue of the fact that both flanges and both thicknesses of the web were connected. The amount of restraint was assumed to result in an effective length factor K_t =0.7. The calculated capacities also assume an effective length factor of 1.0 for weak axis flexural buckling due to the hinged end condition. However, as previously noted, the BG-100 specimens were tested without an actual physical hinge. The rotational restraint provided by the gusset plate stiffness was therefore neglected for these specimens. The conservative effect of this assumption can be seen on the figures.

Unstiffened Angles Bolted Through One Leg

The short BA-40, HBA-40, BC-40, and HBC-40 angles all developed distortions in the bolted leg near the gusset plate connection, resulting in failure. In many cases the failure occurred at loads significantly below the predicted buckling loads. The load transferred into the member by the bolts is initially distributed primarily in the bolted leg only. The bolted leg immediately adjacent to the gusset plate is subjected to a combination of concentrated axial load, and bending caused by the fixity at the connection. This combination of stresses may lead to failure at loads below the calculated buckling loads.

Based on correlation to the experimental test results, the following simple modification is recommended to avoid premature failure of such angles. An upper limit to the compressive strength should be calculated as the product of the yield strength multiplied by the area of the flat portion of the bolted leg for 90° angles, or 90% of the area of the flat portion of the bolted leg for 60° angles. If the local stress distribution in the bolted leg near the connection exceeds the yield stress, the leg begins to buckle, leading to failure. The proposed compressive limit is defined below.

For 90° angles

[1] $$C_{r_{max}} = F_y wt$$

For 60° angles

[2] $$C_{r_{max}} = F_y (0.9w)t$$

where

w	=	flat width of leg
t	=	leg thickness
F_y	=	yield strength

Although the method is simplistic, and does not necessarily account precisely for the actual stress distribution in the vicinity of the connection, it does result in more reasonable ultimate load predictions for very short angles than that provided by any of the design methods. It is therefore recommended that the upper limits defined above be considered in addition to buckling loads defined in the design methods. Table 5 compares the results of BA-40, HBA-40, BC-40, and HBC-40 tests, with the proposed upper compressive limits as defined above. The yield strengths for each section were obtained from tension tests performed on flat portions of sections, at the three temperature levels used in the static compression tests. The calculated compressive limit for each specimen is based on the yield strength measured at the same temperature as the static test. The mean ratio of the experimental failure loads to the upper limit loads calculated for the BA-40, HBA-40, BC-40, and HBC-40 angles is equal to 1.0, and the standard deviation is 0.058.

Figure 14 compares the experimental results with the loads predicted using ASCE Manual 52's recommendations, with two modifications. The first modification includes the proposed limit for short unstiffened angles. The second modification is that the back-to-back channel capacity is modified utilizing the recommendations of CSA-S136. By comparing the data with the 1:1 correspondence line it can be seen that the experimental results are predicted very well by the methods of ASCE Manual 52 (when modified as described above). Data which falls below the 1:1 line indicates unconservative predicted loads, and as evidenced on the figure, such instances are limited in number of occurrences.

Summary, conclusions, and recommendations

A research program was performed at the University of Manitoba to examine the axial load carrying capacity of a number of cold-formed shapes suitable for transmission tower construction. The testing program included a total of 189 axial load tests. The testing was carried out over a fifteen month period. Three different test setups were used in this investigation. Test parameters included: two types of steel, five different shapes, three slenderness ratios, and three temperatures. Specimens were tested in setups designed to simulate end conditions representative of tower members by loading through single legs bolted to gusset plates. Some sections were tested as axially loaded leg members with hinged end conditions. Test results were compared to predicted loads using the Canadian Standards CAN/CSA-S136-M89 Standard for Cold Formed Steel Structural Members, and CAN/CSA-S37-M86 Standard Antennas, Towers, and Antenna Supporting Structures. The ASCE Manual 52 Guide for Design of Steel Transmission Towers, and the ECCS Recommendations for Angles in Lattice Transmission Towers were also used. The following is a summary of the findings:

-The average of all experimental failure loads when tested at 0° C was 1.3 % higher than at room temperature.

-The average of all experimental failure loads when tested at -50° C was 3.8 % higher than at room temperature.

-The amount of load increase at -50° C was the largest for members with L/r = 40. These specimens averaged loads 7.4 % higher than at room temperature. Specimens with L/r = 100 and 200 only showed a 1 to 2 % increase.

Based on the results of the research and analysis, the following recommendations are made:

-Within the test parameters used, cold temperature was not found to be detrimental to the performance of cold-formed sections under static compressive load, and may be neglected in design.

-Caution should be exercised in designing eccentrically loaded unstiffened angles with slenderness ratios of approximately 40. Code prediction reliability was much lower for these sections than for longer sections.

-In general, with the exceptions mentioned, the design methods reviewed in this study provided acceptable results and appear to be generally adequate for design of cold-formed sections for transmission towers.

-The design of short unstiffened angles should be modified to account for the concentration of load in the bolted leg at the connection.

-Back-to-back channels designed according to the ASCE Manual 52 are unconservative, and could be improved by modifying the effective length to account for the spacing of connectors as provided by the CSA-S136 Standard, and by accounting for the reduced Euler buckling capacity due to member imperfections.

-In general, with the exceptions mentioned, the design methods reviewed in this study provided acceptable results and appear to be adequate for the design of cold-formed steel sections for transmission towers. However, ASCE Manual 52 was found by the author to be the preferred guide. The Manual is widely accepted by tower designers, and it's recommendations are supported by numerous laboratory and full-scale tests. In particular, the effective length formulas used to design angles were found to accurately account for both connection eccentricity and end fixity

Acknowledgements

The project described in this paper was sponsored by the Canadian Electrical Association (Project #340 T 844), and by Manitoba Hydro.

References

ASCE-American Society of Civil Engineers, 1988. "Guide for Design of Steel Transmission Towers," ASCE Manuals and Reports on Engineering Practice No. 52, Second Edition, New York, N.Y.

CSA-Canadian Standards Association, 1986. "CAN/CSA-S37-M86, Antennas towers and antenna supporting structures," National Standard of Canada, Rexdale, Ont., Canada.

CSA-Canadian Standards Association, 1989. "CAN/CSA-S16.1-M89, Limit states design of steel structures," National Standard of Canada, Rexdale, Ont., Canada.

CSA-Canadian Standards Association, 1991. "Special Publication S136.1-M-91 Commentary on CAN/CSA-S136-M89, Cold formed steel structural members," National Standard of Canada, Rexdale, Ont., Canada.

CSA-Canadian Standards Association, 1989. "CAN/CSA-S136-M89, Cold formed steel structural members," National Standard of Canada, Rexdale, Ont., Canada.

European Convention for Constructional Steelwork, 1985. "Recommendations for Angles in Lattice Transmission Towers," ECCS - Technical Committee 8 - Structural Stability Technical Working Group 8.1 - Components, First Edition 1985 No. 39, Brussels, Belgium.

Polyzois D., Abdel-Rahim A.B., Charnvarnichborikarn P., "Effect of Galvanizing, Cold-Forming and Subfreezing Temperature on the Mechanical Properties of Cold-Formed Steel," Paper to be presented at the 1994 CSCE Annual Conference, June 2, 1994.

Table 1 Test Parameters

Section	Type of Steel	Nominal Slenderness (L/r)	Length (mm)	Number of tests At each temperature -50°C	0°C	Room Temp.
BA		40	552	3	3	3
		100	1380	3	3	3
		200	2760	3	3	3
BB		40	855	3	3	3
		100	1950	3	3	3
	ASTM	200	4240	3	3	3
BC	A715	40	736	3	3	3
	Grade	100	1840	3	3	3
	60	200	3680	3	3	3
BG		40	1640	3	3	3
		100	4120	3	3	3
		200	8245	0	0	3
BN		40	1640	3	3	3
		100	4105	3	3	3
		200	8210	0	0	3
HBA		40	552	3	0	3
		100	1380	3	0	3
		200	2760	3	0	3
HBB		40	780	3	0	3
	CSA	100	1950	3	0	3
	G40.21	200	3900	3	0	3
HBC	Grade	40	736	3	0	3
	300 W	100	1840	3	0	3
		200	3680	3	0	3
HBN		40	1580	3	0	3
		100	3950	3	0	3
Total				189 tests		

Table 2 Section Properties

Section	A (mm^2)	Ix (10^3 mm^4)	Iy (10^3 mm^4)	J (mm^4)	Cw (mm^6)	rx (mm)	ry (mm)
BA	530	434.34	98.076	2759	0	28.6	13.6
HBA	603	481.08	111.77	4073	0	28.2	13.6
BB	787	1132.30	327.4	5174	331	37.9	20.4
HBB	822	941.66	327.41	5353	190	33.8	19.96
BC	595	345.53	201.38	3173	0	24.1	18.4
HBC	700	423.02	260.14	4725	0	24.6	19.3
BG	1925	3376.65	3318.92	10266	3604	41.9	41.5
BN	2564	5115.00	4394.53	21368	4354	44.7	41.5
HBN	2300	3966.00	3850.02	15531	5538	41.5	40.9

Table 3 Tensile Material Strength (MPa)

Section	Specified Strength	Coupon yield strength Galvanized	Ungalvanized
BA	415	469	424
BB	415	445	418
BC	415	477	434
BG	415	438	419
BN	300	481	434
HBA	300	409	289
HBB	300	418	311
HBC	300	415	315
HBN	300	401	290

Table 4 Ratio of mean experimental failure loads to predicted loads

Section	L/r	Mean Exp. result (kN)	S136	S37	Manual 52	ECCS	S16.1
BA	40	120.0	1.01	0.89	1.00	1.02	(a)
BA	100	101.0	1.19	1.15	1.13	1.29	(a)
BA	200	29.0	1.04	1.21	1.12	1.16	(a)
HBA	40	123.0	0.82	0.73	0.84	0.79	(a)
HBA	100	116.0	1.06	1.10	1.13	1.18	(a)
HBA	200	30.0	0.91	1.07	1.00	1.07	(a)
BB	40	214.9	1.09	(a)	1.15	(a)	(a)
BB	100	134.6	1.12	(a)	1.18	(a)	(a)
BB	200	46.3	1.19	(a)	1.25	(a)	(a)
HBB	40	197.3	0.88	(a)	1.03	(a)	(a)
HBB	100	126.7	0.86	(a)	1.01	(a)	(a)
HBB	200	46.0	0.98	(a)	1.05	(a)	(a)
BC	40	119.0	1.02	0.95	0.98	(a)	(a)
BC	100	95.1	1.11	1.07	1.01	(a)	(a)
BC	200	32.8	1.06	1.17	1.09	(a)	(a)
HBC	40	118.5	0.81	0.72	0.78	(a)	(a)
HBC	100	105.3	0.95	0.91	0.89	(a)	(a)
HBC	200	39.0	0.98	1.08	1.00	(a)	(a)
BG	40	786.3	1.20	(a)	1.14	(a)	(a)
BG	100	470.4	1.83	(a)	1.52	(a)	(a)
BG	200	94.0	1.31	(a)	1.08	(a)	(a)
BN	40	1073.9	1.03	(a)	1.00	(a)	1.13
BN	100	410.6	1.18	(a)	0.85	(a)	1.16
BN	200	79.7	0.90	(a)	0.64	(a)	0.76
HBN	40	793.0	0.99	(a)	0.95	(a)	1.06
HBN	100	337.2	1.04	(a)	0.74	(a)	1.08

(a) : capacities were not calculated for these sections

Table 5 Proposed upper limit capacity for short unstiffened angles loaded through one leg

Section	Test Temp. (°C)	Coupon Yield (MPa)	Test Load (kN)	Cr limit (kN	Test load / Cr limit
BA-40-1	23	469	113	112.7	1.00
BA-40-2	23	469	126	112.7	1.12
BA-40-3	23	469	120	112.7	1.06
BA-40-18	23	469	118	112.7	1.05
BA-40-19	23	469	120	112.7	1.06
BA-40-4	0	486	116	116.8	0.99
BA-40-5	0	486	125	116.8	1.07
BA-40-6	0	486	116	116.8	0.99
BA-40-7	-50	519	122	124.8	0.98
BA-40-8	-50	519	110	124.8	0.88
BA-40-9	-50	519	123	124.8	0.99
BA-40-19	-50	519	127	124.8	1.02
HBA-40-1	23	409	115	113.9	1.01
HBA-40-2	23	409	118	113.9	1.04
HBA-40-3	23	409	120	113.9	1.05
HBA-40-4	-50	511	131	142.3	0.92
HBA-40-5	-50	511	129	142.3	0.91
HBA-40-6	-50	511	124	142.3	0.87
BC-40-1	23	477	116	112.5	1.03
BC-40-2	23	477	121	112.5	1.08
BC-40-3	23	477	116	112.5	1.03
BC-40-4	0	488	119	115.1	1.03
BC-40-5	0	488	124	115.1	1.08
BC-40-6	0	488	120	115.1	1.04
BC-40-7	-50	510	125	120.3	1.04
BC-40-8	-50	510	119	120.3	0.99
BC-40-9	-50	510	113	120.3	0.94
HBC-40-1	23	415	110	118.4	0.93
HBC-40-2	23	415	117	118.4	0.99
HBC-40-3	23	415	119	118.4	1.00
HBC-40-4	-50	440	119	125.5	0.95
HBC-40-5	-50	440	120	125.5	0.96
HBC-40-6	-50	440	126	125.5	1.00
				Mean:	1.00
				Standard deviation:	0.058

* Obtained from tension coupons tested at room temp., 0°C, and -50°

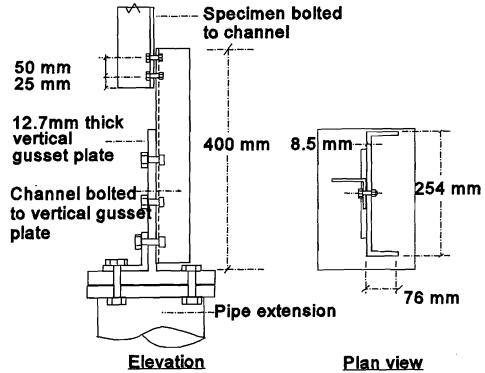

Fig. 1 Schematic of Gusset Plate for Angle Connections

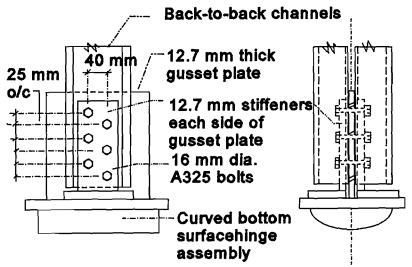

Fig. 2 Schematic of (H)BN Gusset Plate: Setup #1

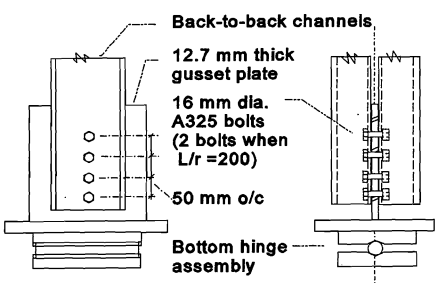

Fig. 3 Schematic of (H)BN Gusset Plate: Setup #2 & #3

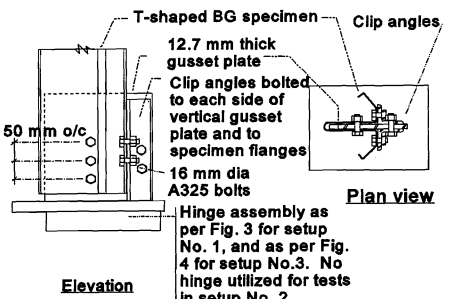

Fig. 4 Schematic of Gusset Plate for BG Connections

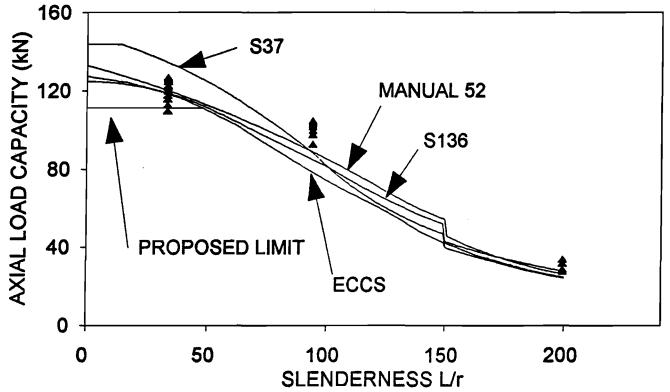

Fig. 5 BA Section Analysis

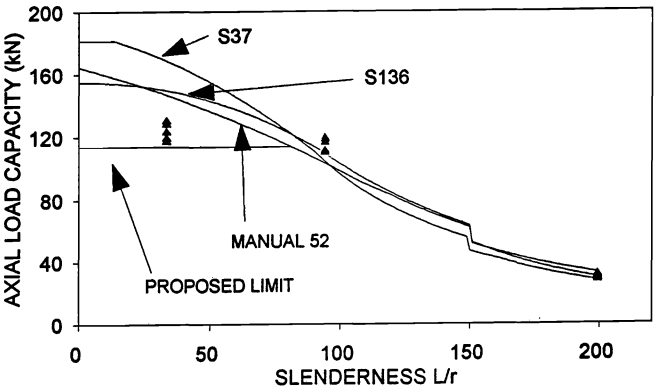

Fig. 6 HBA Section Analysis

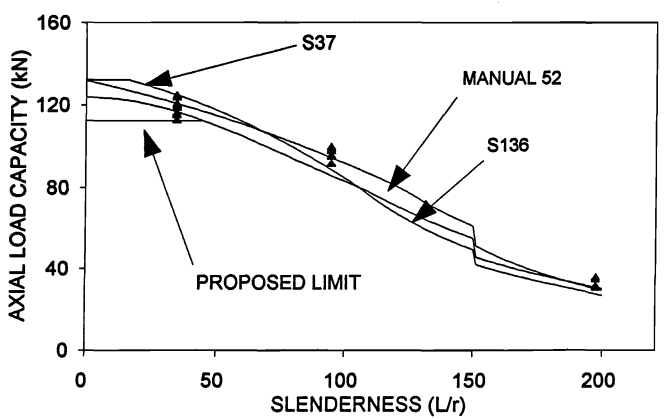

Fig. 7 BC Section Analysis

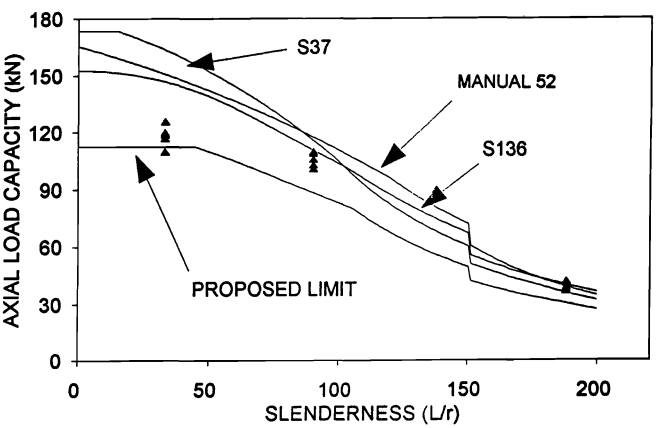

Fig. 8 HBC Section Analysis

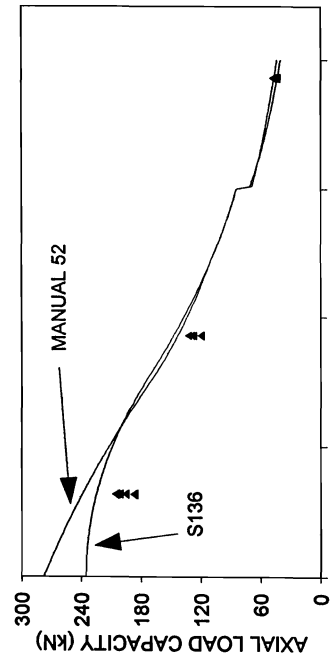

Fig. 10 HBB Section Analysis

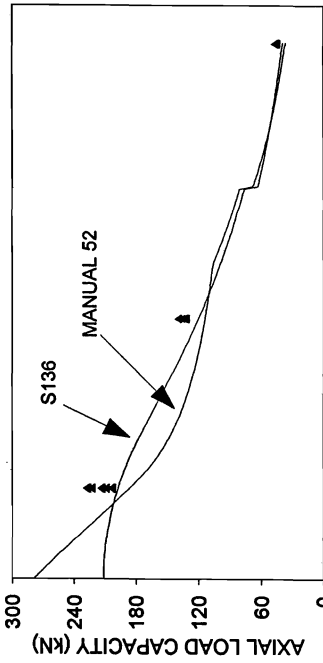

Fig. 9 BB Section Analysis

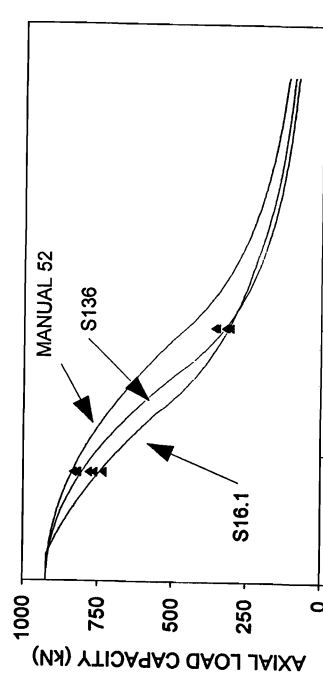

Fig. 12 HBN Section Analysis

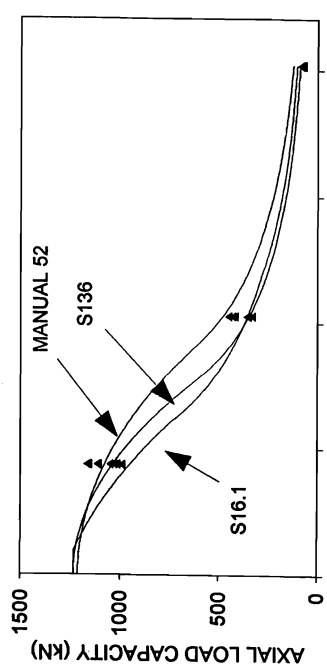

Fig. 11 BN Section Analysis

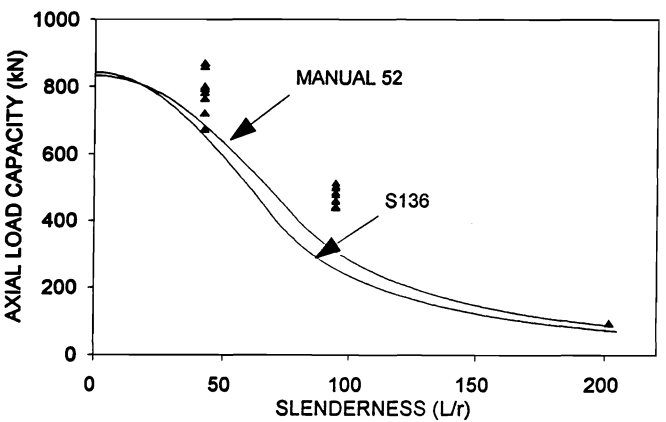

Fig. 13 BG Section Analysis

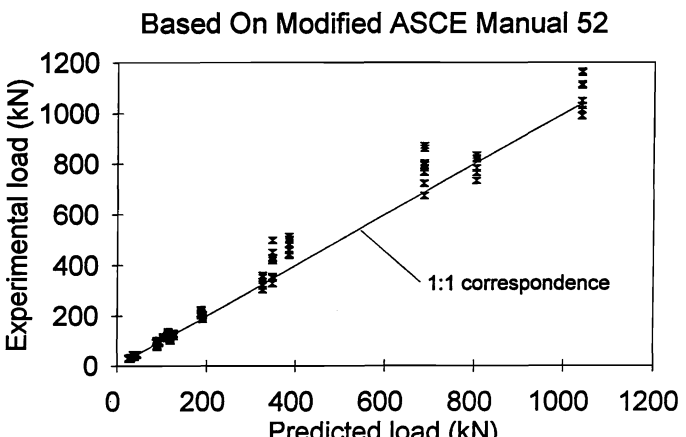

Fig. 14 Comparison of results to modified ASCE Manual 52 Predicted load